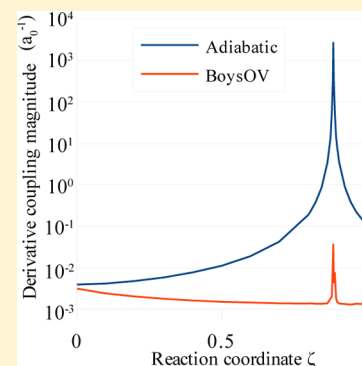


Analysis of Localized Diabatic States beyond the Condon Approximation for Excitation Energy Transfer Processes

Ethan C. Alguire,[†] Shervin Fatehi,[‡] Yihan Shao,[¶] and Joseph E. Subotnik^{*,†}[†]Department of Chemistry, University of Pennsylvania, 231 South 34th Street, Philadelphia, Pennsylvania 19104-6323, United States[‡]Department of Chemistry, University of Utah, 315 South 1400 East, Room 2020, Salt Lake City, Utah 84112-0850, United States[¶]Q-Chem, Inc., 6601 Owens Drive, Suite 105, Pleasanton, California 94588, United States

ABSTRACT: In a previous paper [Fatehi, S.; et al. *J. Chem. Phys.* **2013**, *139*, 124112], we demonstrated a practical method by which analytic derivative couplings of Boys-localized CIS states can be obtained. In this paper, we now apply that same method to the analysis of triplet–triplet energy transfer systems studied by Closs and collaborators [Closs, G. L.; et al. *J. Am. Chem. Soc.* **1988**, *110*, 2652]. For the systems examined, we are able to conclude that (i) the derivative coupling in the BoysOV basis is negligible, and (ii) the diabatic coupling will likely change little over the configuration space explored at room temperature. Furthermore, we propose and evaluate an approximation that allows for the inexpensive calculation of accurate diabatic energy gradients, called the “strictly diabatic” approximation. This work highlights the effectiveness of diabatic state analytic gradient theory in realistic systems and demonstrates that localized diabatic states can serve as an acceptable approximation to strictly diabatic states.



1. INTRODUCTION

The ability to properly model nonadiabatic dynamics is essential for understanding innumerable chemical systems.¹ Problems in the field of nonadiabatic dynamics are commonly approached, at least in a conceptual framework, from the perspective of the strictly diabatic electronic representation. Strictly diabatic wave functions ($\{|\Xi_A\rangle\}$) are defined by the characteristic that they are not coupled to each other by nuclear momenta, or in other words, that the derivative couplings (DCs) are zero

$$d_{AB}^{[Q]} = \langle \Xi_A | \nabla_Q | \Xi_B \rangle = 0 \quad (1)$$

where Q indexes a nuclear degree of freedom. While they are not coupled by nuclear momentum, diabatic states are coupled by elements of the electronic Hamiltonian (H_{AB}) called diabatic couplings. If this Hamiltonian is diagonalized, of course, one obtains the adiabatic basis of electronic states. The cost of this transformation is that the DCs in the new basis are inversely proportional to the energy difference between the states that they couple ($d_{ij}^{[Q]} \propto (E_j - E_i)^{-1}$) and can therefore become large near avoided crossings and diverge near conical intersections. For a brief review of the representation dependence of DCs within the spin boson model, see Appendix A.

While a strictly diabatic basis would be useful, in practice, it is impossible to obtain.^{2,3} In its place, numerous approximations (called simply “diabatic” states) have been proposed. One approach is to directly minimize DCs along a given reaction path.⁴ In more recent years, Yarkony has proposed a method that can minimize DCs for small- to medium-sized systems.^{5,6} Other methods approximate diabatic states by constructing a

basis in which the states change little with respect to nuclear motion; such methods include Pacher, Cederbaum, and Köppel’s block diagonalization;⁷ Atchity, Ruedenberg, et al.’s configurational uniformity;^{8,9} and Nakamura and Truhlar’s fourfold way.^{10–12} Still other techniques approach the problem more obliquely; the generalized Mulliken–Hush (GMH) algorithm of Cave and Newton^{13,14} approximates diabatic states as eigenstates of a component of the dipole operator, utilizing the heuristic property that diabatic states for electron transfer (ET) processes tend to be localized in space. The idea that singular DCs could be removed by obtaining the eigenstates of an observable was later formally demonstrated by Yarkony.^{15–17} Last, there is a plethora of techniques that produce diabatic states by localizing wave functions, including Voityuk’s fragment charge difference (FCD) method;¹⁸ Hsu’s extension of FCD to excitation energy transfer (EET) systems, fragment excitation difference (FED);^{19–21} and Boys and ER localization.^{22–24} The concept of charge localization in ET states was also applied to the construction of diabatic densities in the context of density functional theory (DFT) by Van Voorhis et al.^{25–27} For comprehensive reviews on this topic, see refs 3 and 28. The current work is concerned with localized diabaticization schemes,^{22–24,29} for which diabatic ET and EET states can be approximated by a linear combination of adiabatic states determined by minimizing a functional of the electronic subspace. Hereafter, any reference to diabatic states will refer to localized diabatic states.

Special Issue: David R. Yarkony Festschrift

Received: November 11, 2013

Revised: December 26, 2013

As discussed in previous publications,^{29,30} localized diabatic states could potentially be used with several nonadiabatic dynamics methods,^{31,32} especially those that are agnostic to electronic representation.^{33–36} In order to propagate dynamics in a localized diabatic representation, it is necessary to have an efficient way to determine diabatic gradient quantities; it would be even better to establish that DCs in such a representation are negligible for a particular system. Additionally, localized diabatization methods have been used in the context of Marcus theory to accurately model²⁴ the rate of triplet–triplet EET in systems studied by Closs et al.^{37,38} While theoretical and experimental results agreed reasonably well, until now, we have not been able to prove beyond doubt that this success was not coincidental. After all, Marcus theory is formally applicable only to strictly diabatic states.

In this article, we use our newly developed analytic gradient theory for diabatic states³⁰ to reexamine the validity of locally diabatic states and to ascertain definitively whether the Closs systems conform to the approximations of Marcus theory. With these considerations in mind, first, we compare the DCs of these molecules in the adiabatic and diabatic representations. If the diabatic states are similar to the strictly diabatic states postulated by Marcus, one should expect that their DCs are insignificant even near avoided crossings. Second, we use diabatic Hamiltonian gradients to estimate how much the diabatic coupling changes within the configuration space available to these systems at room temperature. In addition to assuming strictly diabatic states, Marcus theory assumes the Condon approximation, which posits that the diabatic couplings do not change significantly, and we show that it holds true here. Third and finally, in the Discussion section, we will present and evaluate an approximation that can produce diabatic state gradient quantities at the cost of producing adiabatic DCs.

2. NOTATION

The upper case letters $\{I, J, K, L\}$ index adiabatic electronic states, while $\{A, B, C\}$ are used to index diabatic electronic states. The lower case letters $\{i, j\}$ index occupied molecular orbitals, while $\{a, b\}$ index virtual molecular orbitals. Following the convention established in ref 39, nuclear degrees of freedom in the Cartesian basis are indexed by the letter Q , and gradients with respect to such degrees of freedom are denoted by a superscript Q enclosed in square brackets, such as $f^{[Q]}$. Nuclear degrees of freedom in the basis of normal modes are indexed by the letter η , and gradients are similarly represented as superscripts enclosed in brackets, for example, $f^{[\eta]}$. Diabatic states are denoted $|\Xi\rangle$, adiabatic states are denoted $|\Phi\rangle$, and DCs are denoted $d_{ij}^{[Q]}$. All other terms are explained as they arise.

3. THEORY

A. Localized Diabatization. The localized diabatization method is an inexpensive, black box method for generating a diabatic electronic basis as a linear combination of adiabatic states. Localized diabatic states are obtained by mixing a basis of M adiabatic states via an adiabatic-to-diabatic transformation matrix \mathbf{U} , such that

$$|\Xi_A\rangle = \sum_{I=1}^M U_{AI} |\Phi_I\rangle \quad (2)$$

where \mathbf{U} is chosen (1) to be unitary, ensuring orthonormal diabat, and (2) to maximize some diabatization function.

Three such functions, GMH, Boys, and BoysOV, are defined in terms of state dipole operators; therefore, their respective analytic gradient expressions have many similarities, which will be described below. Diabatic states in the GMH representation must have a dipole operator that is diagonalized in the direction of charge transfer.¹³ Boys diabatization represents an extension of this method to multiple centers of charge and in fact reduces to GMH for two-state systems.²² In principle, Boys diabatic states can be thought of as adiabatic states perturbed by the approximate effects of a strongly localizing solvent bath, one that exerts a linear electrostatic potential on the electronic system being diabatized. Consequently, maximizing this interaction is equivalent to maximizing the localization function f_{Boys} given by

$$f_{\text{Boys}}(\mathbf{U}) = f_{\text{Boys}}(\{\Xi_A\}) \quad (3)$$

$$= \sum_{A,B=1}^M |\langle \Xi_A | \boldsymbol{\mu} | \Xi_A \rangle - \langle \Xi_B | \boldsymbol{\mu} | \Xi_B \rangle|^2 \quad (4)$$

where $\boldsymbol{\mu}$ is the electronic dipole operator. Boys diabatic states are useful for localizing ET states but are subject to certain limitations. In particular, the Boys method is unable to localize the electronic states of an EET system, in which electronic excitation, not charge, becomes localized. In an alternative method, called BoysOV localization,²⁴ uses a diabatization function given by

$$f_{\text{BoysOV}}(\mathbf{U}) = \sum_{A,B=1}^M |\langle \Xi_A | \boldsymbol{\mu}^{\text{occ}} | \Xi_A \rangle - \langle \Xi_B | \boldsymbol{\mu}^{\text{occ}} | \Xi_B \rangle|^2 \quad (5)$$

$$+ \sum_{A,B=1}^M |\langle \Xi_A | \boldsymbol{\mu}^{\text{virt}} | \Xi_A \rangle - \langle \Xi_B | \boldsymbol{\mu}^{\text{virt}} | \Xi_B \rangle|^2 \quad (6)$$

where the dipole operators $\boldsymbol{\mu}^{\text{occ}}$ and $\boldsymbol{\mu}^{\text{virt}}$ only interact with occupied and virtual orbital densities, respectively. For CIS states, this means

$$\langle \Xi_A | \boldsymbol{\mu}^{\text{occ}} | \Xi_B \rangle = \boldsymbol{\mu}_{AB}^{\text{occ}} = - \sum_{i,j,a} t_i^{A,a} t_j^{B,a} \boldsymbol{\mu}_{ij} \quad (7)$$

and

$$\langle \Xi_A | \boldsymbol{\mu}^{\text{virt}} | \Xi_B \rangle = \boldsymbol{\mu}_{AB}^{\text{virt}} = \sum_{i,a,b} t_i^{A,a} t_i^{B,b} \boldsymbol{\mu}_{ab} \quad (8)$$

where we have introduced CIS amplitudes $\{t\}$. By separately localizing these two types of electron densities, BoysOV allows for the localization of excitations for a given set of states, even if charge cannot be localized for the same subspace. Formally, BoysOV can be easily applied to CIS or time-dependent density functional theory under the Tamm–Dancoff approximation (TD-DFT/TDA), but further generalizations are possible (see Appendix B).

B. DCs between Localized Diabatic States. The formal expression for DCs between localized diabatic states can be written simply as

$$d_{AB}^{[Q]} = \sum_{IJ} U_{AI} d_{IJ}^{[Q]} U_{BJ} + \sum_I U_{AI} U_{BI}^{[Q]} \quad (9)$$

Expressions for the DCs^{40–48} and gradients^{49–53} of CI adiabatic states are available, and we have described methods

for obtaining analytic DCs between adiabatic states within the CIS formalism.³⁹ Calculating any gradient quantity within a diabatic representation also requires the transformation matrix gradient, $\mathbf{U}^{[Q]}$. The process for calculating $\mathbf{U}^{[Q]}$ for Boys diabatic states is described in detail in ref 30. Here, we will broadly describe the process for the three localized diabaticization schemes that make use of dipole operators: GMH, Boys, and BoysOV localization. In each case, there are two groups of constraints on the diabatic states that can be used to construct a supermatrix equation

$$\sum_{CK} \begin{bmatrix} \mathcal{A}_{ABCK} \\ \mathcal{B}_{ABCK} \end{bmatrix} \mathbf{U}_{CK}^{[Q]} = - \begin{bmatrix} 0 \\ \mathbf{C}_{AB}^{[Q]} \end{bmatrix} \quad (10)$$

which can subsequently be solved to obtain $\mathbf{U}^{[Q]}$. The first set of constraints

$$\sum_{CK} \mathcal{A}_{ABCK} \mathbf{U}_{CK}^{[Q]} = 0 \quad (11)$$

arises from the condition that diabatic states must be orthonormal

$$\sum_I U_{AI} U_{BI} = \delta_{AB} \quad (12)$$

If we take the gradient of eq 12 with respect to nuclear degrees of freedom Q , we obtain

$$\sum_I U_{AI}^{[Q]} U_{BI} + \sum_I U_{AI} U_{BI}^{[Q]} = 0 \quad (13)$$

which holds for all state pairs $A \geq B$. This result can be rearranged in the form of eq 11, where $\mathcal{A}_{ABCK} = \delta_{AC} U_{BK} + \delta_{BC} U_{AK}$.

While the unitarity condition is true for all localized diabaticization schemes, in order to fully define the M^2 elements of $\mathbf{U}^{[Q]}$, we must turn to the second set of constraints

$$\sum_{CK} \mathcal{B}_{ABCK} \mathbf{U}_{CK}^{[Q]} = -\mathbf{C}_{AB}^{[Q]} \quad (14)$$

which involve conditions specific to each scheme. By definition,¹³ GMH states must be constructed such that for $M = 2$

$$\boldsymbol{\mu}_{AB} \cdot (\boldsymbol{\mu}_{11} - \boldsymbol{\mu}_{22}) = 0 \quad (15)$$

where $\boldsymbol{\mu}_{11}$ and $\boldsymbol{\mu}_{22}$ are diagonal elements of the dipole operator in the adiabatic basis, localized on the two different charge centers associated with the ET reaction. Taking the gradient of eq 15 with respect to nuclear degrees of freedom Q again allows us to express $\mathbf{U}^{[Q]}$ in the context of a supermatrix equation (eq 14), for which

$$\mathcal{B}_{ABCK}^{\text{GMH}} = \delta_{AC} \boldsymbol{\mu}_{BK} \cdot (\boldsymbol{\mu}_{11} - \boldsymbol{\mu}_{22}) + \delta_{BC} \boldsymbol{\mu}_{AK} \cdot (\boldsymbol{\mu}_{11} - \boldsymbol{\mu}_{22}) \quad (16)$$

and

$$\mathbf{C}_{AB}^{\text{GMH}[Q]} = \sum_{IJ} [\boldsymbol{\mu}_{IJ}^{[Q]} \cdot (\boldsymbol{\mu}_{11} - \boldsymbol{\mu}_{22}) + \boldsymbol{\mu}_{IJ} \cdot (\boldsymbol{\mu}_{11}^{[Q]} - \boldsymbol{\mu}_{22}^{[Q]})] U_{AI} U_{BJ} \quad (18)$$

A similar approach is used to define the constraints on $\mathbf{U}^{[Q]}$ for the Boys representation. It can be shown²² that the condition

$$\boldsymbol{\mu}_{AB} \cdot (\boldsymbol{\mu}_{AA} - \boldsymbol{\mu}_{BB}) = 0 \quad (19)$$

must be obeyed for all state pairs such that $A > B$. The gradient of this expression can then be taken, and the result can be written in the form of eq 14 with

$$\begin{aligned} \mathcal{B}_{ABCK}^{\text{Boys}} &= \delta_{AC} [2\boldsymbol{\mu}_{AB} \cdot \boldsymbol{\mu}_{KA} + (\boldsymbol{\mu}_{AA} - \boldsymbol{\mu}_{BB}) \cdot \boldsymbol{\mu}_{KB}] \\ &\quad - \delta_{BC} [2\boldsymbol{\mu}_{AB} \cdot \boldsymbol{\mu}_{KB} - (\boldsymbol{\mu}_{AA} - \boldsymbol{\mu}_{BB}) \cdot \boldsymbol{\mu}_{KA}] \end{aligned} \quad (20)$$

and

$$\begin{aligned} \mathbf{C}_{AB}^{\text{Boys}[Q]} &= \sum_{IJKL} [\boldsymbol{\mu}_{IJ}^{[Q]} \cdot \boldsymbol{\mu}_{KL} + \boldsymbol{\mu}_{IJ} \cdot \boldsymbol{\mu}_{KL}^{[Q]}] U_{AI} U_{BJ} \\ &\quad \times (U_{AK} U_{AL} - U_{BK} U_{BL}) \end{aligned} \quad (22)$$

We can easily extend the form of this supermatrix expression to BoysOV localization if we instead require that the condition

$$\boldsymbol{\mu}_{AB}^{\text{occ}} \cdot (\boldsymbol{\mu}_{AA}^{\text{occ}} - \boldsymbol{\mu}_{BB}^{\text{occ}}) + \boldsymbol{\mu}_{AB}^{\text{virt}} \cdot (\boldsymbol{\mu}_{AA}^{\text{virt}} - \boldsymbol{\mu}_{BB}^{\text{virt}}) = 0 \quad (23)$$

must be satisfied. This “BoysOV condition” is simply the Boys condition divided into separate parts for the occupied and virtual contributions to the dipole operator. The resulting supermatrices, represented as functions of the dipole operators, can be written

$$\mathcal{B}^{\text{BoysOV}} = \mathcal{B}^{\text{Boys}}(\boldsymbol{\mu}^{\text{occ}}) + \mathcal{B}^{\text{Boys}}(\boldsymbol{\mu}^{\text{virt}}) \quad (24)$$

and

$$\mathbf{C}^{\text{BoysOV}[Q]} = \mathbf{C}^{\text{Boys}[Q]}(\boldsymbol{\mu}^{\text{occ}}) + \mathbf{C}^{\text{Boys}[Q]}(\boldsymbol{\mu}^{\text{virt}}) \quad (25)$$

The supermatrices necessary for obtaining $\mathbf{U}^{[Q]}$ exist in a small-dimensional state space; therefore, inverting eq 10 is computationally trivial. The costly part of obtaining diabatic gradient quantities is filling in the constraint matrix $\mathbf{C}^{[Q]}$ with adiabatic dipole gradients $\boldsymbol{\mu}^{[Q]}$. Note that although the cost of calculating $\mathbf{C}^{[Q]}$ for GMH is equivalent to the same procedure for Boys diabatic states, the cost for BoysOV is twice as great as each quantity must be calculated once for virtual densities and once for occupied densities. Consequently, for a two-state calculation, the cost of this procedure for BoysOV states should be approximately 20 times the cost of a CIS gradient.³⁰

C. Diabatic Hamiltonian Gradient and the Strictly Diabatic Approximation. In addition to producing diabatic-basis DCs, the transformation matrix gradient $\mathbf{U}^{[Q]}$ can be used to produce any diabatic gradient quantity. Among these quantities, the diabatic Hamiltonian gradient $\mathbf{H}^{[Q]}$ is of primary interest. As with the expression for the DC (eq 9), the expression for the Hamiltonian gradient is simple

$$\mathbf{H}_{AB}^{[Q]} = \sum_{IJ} (U_{AI} H_{IJ}^{[Q]} U_{BJ} + U_{AI}^{[Q]} H_{IJ} U_{BJ} + U_{AI} H_{IJ} U_{BJ}^{[Q]}) \quad (26)$$

From eq 26, one can calculate both energy gradients (diagonal elements) and diabatic coupling derivatives (off-diagonal elements). The gradients of any other observable can be represented by the same expression by simply replacing the Hamiltonian with the Hermitian operator of interest.

As for DCs, the most costly step in evaluating eq 26 is the calculation of $\mathbf{U}^{[Q]}$. Reducing the cost of building the energy gradients much less expensive and therefore practical for larger molecules. One shortcut, which we dub the “strictly diabatic” approximation, takes advantage of one of the principal desired properties of diabatic states, negligible DCs. Formally assuming

the strictly diabatic condition (eq 1) allows us to solve eq 9 for $U^{[Q]}$

$$U_{Ai}^{[Q]} = \sum_j U_{Aj} d_{ji}^{[Q]} \quad (27)$$

If it can be demonstrated that localized diabatic states have small enough DCs to make this a viable approximation, diabatic gradient quantities could be obtained for the cost of adiabatic DCs, which would reduce calculation time by an order of magnitude. Furthermore, because eq 9 does not require any information about the diabatic basis beyond the transformation matrix, it can be trivially applied to any localized diabatization method.

4. RESULTS

All results were calculated using a development version of the Q-CHEM software package.^{54,55} Excited states were generated using the restricted Hartree–Fock configuration interaction singles (RHF-CIS) formalism with a 6-31G** basis set. The systems under consideration are similar to those used in ref 37; each is a donor–bridge–acceptor (DBA) molecule in which a 4-benzaldehydeyl donor and a 2-naphthyl acceptor are joined to a variable bridge. Note that in the actual experiments, the donor is a benzophenoneyl group instead of a benzaldehydeyl group. We designate these molecules using the same naming scheme as that employed in ref 37; for example, C-1,3ea signifies a cyclohexane bridge to which the donor group is attached at carbon 1 equatorially and to which the acceptor group is attached to carbon 3 axially. One such molecule, C-1,4ee, is pictured in Figure 1. The electronic subspace is restricted to the

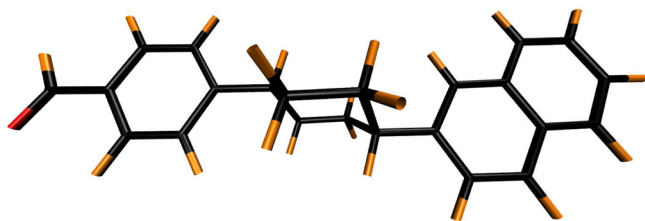


Figure 1. The DBA molecule C-1,4ee has two minima on the T_1 surface associated with a triplet–triplet EET system. In the higher-energy local minimum configuration, the excitation is localized on the benzaldehydeyl donor (the AD^* state). In the global minimum configuration for this surface, the excitation is localized on the 2-naphthyl acceptor (the A^*D state). Here, C-1,4ee is shown in the geometry optimized for the A^*D configuration of the T_1 excited state.

T_1 and T_2 excited states for each molecule. The space of configurations considered is a reaction coordinate ζ defined as a linear interpolation between the “before” and “after” configurations of a triplet–triplet EET reaction, that is, the A^*D ($\zeta = 0$) and AD^* ($\zeta = 1$) energy-minimized geometries of the T_1 state. Diabatic states are constructed in the BoysOV representation. Normal modes are indexed by frequency, where mode 1 is the lowest-frequency mode.

A. DC in the BoysOV Representation. While the DC is of course a $3N$ vector, for the purposes of analyzing the validity of eq 1 for localized diabatic states, it is sufficient to discuss the DC magnitudes alone. Because the systems under consideration are involved in energy transfer and not charge transfer, the only localized diabatization method considered here is BoysOV. DC magnitudes in the adiabatic and BoysOV representations for C-1,4ee are shown in Figure 2. This system

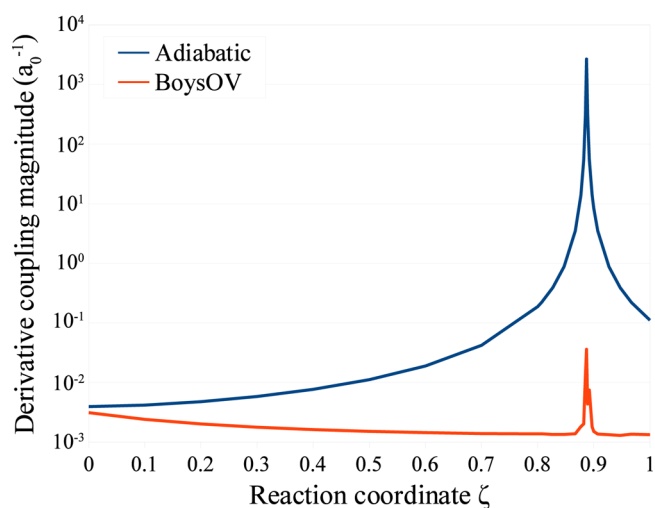


Figure 2. Magnitudes of the DC vector along the linearly interpolated reaction pathway between A^*D ($\zeta = 0$) and AD^* ($\zeta = 1$) T_1 states of the C-1,4ee molecule. DC magnitudes are presented in both the adiabatic and diabatic (BoysOV) bases. While the DC magnitude is smaller in the BoysOV basis for every point sampled, the degree of reduction is greatest near the avoided crossing, where it peaks at $2.7 \times 10^3 a_0^{-1}$ in the adiabatic basis, and $3.6 \times 10^{-2} a_0^{-1}$ in the diabatic basis. There is little difference between the adiabatic and diabatic representations far from the avoided crossing at $\zeta = 0$, where DC magnitudes are negligible in either representation.

is typical of the molecules considered in this study; the adiabatic DC magnitudes tend to be negligible near the end points of the reaction coordinate but peak sharply near the avoided crossing.

By contrast, in the case of diabatic states, the DC magnitude is universally smaller in the BoysOV representation than it is in the adiabatic representation, particularly near the avoided crossing, where it is smaller by a factor of nearly 10^5 . Just like the corresponding adiabatic quantity, the BoysOV DC magnitude peaks near the avoided crossing. However, it is not clear whether this peak is an accurate reflection of the BoysOV wave function behavior in this region; the coupled-perturbed CIS (CPCIS) equations necessary for calculating BoysOV DCs are particularly unstable here, requiring relaxed convergence criteria. Furthermore, the final expression for the diabatic DC near an avoided crossing involves two very large terms of opposite sign, the conjugated adiabatic DC and the rotation matrix gradient (cf. eq 9). As a result, numerical noise may become significant when the adiabatic DC magnitude becomes large. However, it should be noted that the expression for the adiabatic DCs is not affected by the same instabilities; therefore, these can be generated at full precision near the avoided crossing. Despite the higher error associated with calculating the diabatic DCs, their magnitude is still universally small, peaking at a value of $0.036 a_0^{-1}$.

For a more general comparison, we have collected the magnitudes of the DCs for several Closs systems near the avoided crossing point along the chosen reaction coordinate. This information is presented in Table 1. As in the case of C-1,4ee, the avoided crossing point is where the DC magnitude peaks in each representation. In the diabatic representation, the DC magnitude is reduced from the corresponding adiabatic value by at least 4 orders of magnitude in each case and is never greater than $0.1 a_0^{-1}$. As mentioned for the C-1,4ee system, it seems likely that the true DC magnitudes for BoysOV states

Table 1. Magnitudes of DCs between the Triplet–Triplet Energy Transfer States of Three Different Closs Molecules in the Adiabatic and Diabatic (BoysOV) Representations at the Configuration Nearest to the Avoided Crossing along the Linearly Defined Reaction Coordinate ζ^a

representation	DC magnitude at avoided crossing point (a_0^{-1})		
	C-1,3ea	C-1,3ee	C-1,4ee
adiabatic	2500	970	2700
diabatic	0.066	0.0078	0.036
A/D ratio	3.8×10^4	1.2×10^5	7.4×10^4

^aThese configurations represent the maximum DC magnitudes among the configurations sampled for each system, suggesting that the diabatic DCs are negligible over all relevant portions of configuration space for these systems.

are even smaller than the values presented here as instabilities in the orbital response calculations and finite precision error have likely inflated the size of this quantity near the avoided crossings.

B. Evaluating Fluctuations in the Diabatic Coupling.

While the DCs in the adiabatic representation appear to be tightly localized in space for these systems, the same is not necessarily true for the diabatic coupling in the BoysOV representation. On the contrary, the diabatic coupling varies little along the reaction coordinate sampled in our study (Figure 3); the difference between its maximum and minimum values is only 7%. At first glance, Figure 3 would seem to

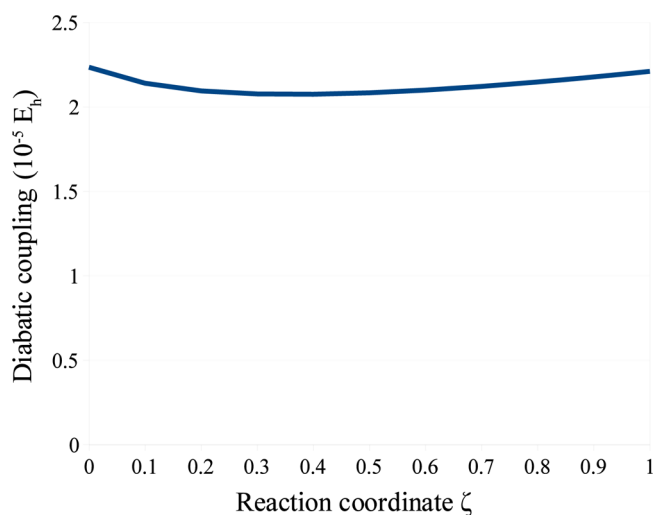


Figure 3. Diabatic coupling along the linearly interpolated reaction pathway between A*D ($\zeta = 0$) and AD* ($\zeta = 1$) T₁ states of the C-1,4ee molecule in the BoysOV representation. Among the points sampled, the maximum value (22.4 μE_h) and minimum value (20.8 μE_h) differ only by about 7% over the extent of the points sampled here; changing $\zeta = 0$ to $\zeta = 1$ constitutes a change of 0.88 a_0 .

conform to the Condon approximation for this molecular system and thus to the assumptions of Marcus theory (as explained in refs 56 and 57). Nevertheless, Figure 3 is only a one-dimensional representation of the diabatic coupling. To understand multidimensional effects, in Figure 4, we plot the norm of the diabatic coupling gradient ($|H_{AB}^{[Q]}|$, for $A \neq B$) as a function of the reaction coordinate. Although $|H_{AB}^{[Q]}|$ overlaps little with the reaction coordinate, should the molecule be displaced into some orthogonal mode, the diabatic coupling

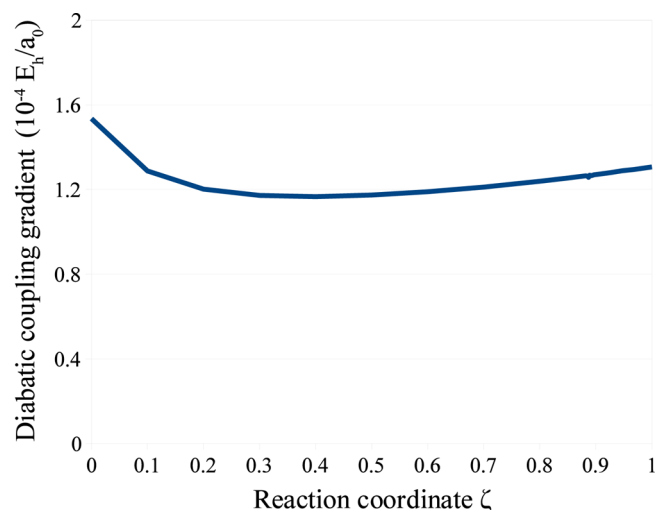


Figure 4. Magnitude of the diabatic coupling gradient ($|H_{AB}^{[Q]}|$) along the linearly interpolated reaction pathway between A*D ($\zeta = 0$) and AD* ($\zeta = 1$) T₁ states of the C-1,4ee molecule in the BoysOV representation. The magnitude of the gradient alone suggests that the diabatic couplings change by as much as 140 μE_h over the reaction pathway defined here (total length of 0.88 a_0); however, as the graph of the diabatic coupling makes clear (Figure 3), the diabatic coupling gradient overlaps little with the degree of freedom defined by the reaction coordinate.

will not necessarily remain stable. Thus, it is worthwhile to explore whether this molecule is rigid enough at room temperature to avoid such conformational fluctuations as might change its diabatic coupling significantly.

To determine how much the diabatic coupling of this molecule might deviate due to conformational fluctuations, we must first estimate the probable conformational changes accessible to it at room temperature and then combine this information with the diabatic coupling gradient. We can accomplish this goal in three steps: (1) For each minimum-energy geometry on the T₁ surface, we approximate the shape of the potential well as that of the minimum-energy ground-state configuration. We can then use a Hessian calculation at the S₀ minimum-energy configuration to describe the normal modes and corresponding vibrational frequencies (ν_η) of the system. (2) We approximate the magnitude of configurational fluctuations (ΔL_η) with respect to this degree of freedom by taking the square root of the thermal average of the squared displacement operators along these modes

$$\Delta L_\eta = \sqrt{\sum_m P_m \Delta X_{\eta,m}^2} = \sqrt{\sum_m P_m \langle \phi_m | \hat{X}_\eta^2 | \phi_m \rangle} \quad (28)$$

where ϕ_m is the m th harmonic oscillator stationary state and P_m is the corresponding Boltzmann-weighted probability at $T = 298$ K. (3) We estimate the change in diabatic coupling with respect to this degree of freedom ($\Delta H_{AB,\eta}$) as the product of the component of the gradient along this degree of freedom with the magnitude of the fluctuation along this degree of freedom, $\Delta H_{AB,\eta} = \Delta L_\eta H_{AB}^{[\eta]}$.

Using this procedure, we can calculate $\Delta H_{AB,\eta}$ across all degrees of freedom by examining the projection of the gradient vectors onto each normal mode of the ground state. For the $\zeta = 0$ configuration, we find that there are five modes along which the diabatic coupling could change by more than 20% of its

reference value. The most significant of these is mode 59; our analysis suggests that the diabatic coupling could change by 33% if the molecule were to move along this degree of freedom at room temperature. For the $\zeta = 1$ configuration, there are only three modes that the diabatic coupling could change by more than 20%; mode 59 is also the most significant in this case, along which the diabatic coupling can change by 31%. For a visual representation of the normal modes that correspond to the greatest change in the diabatic coupling, see Figure 5.

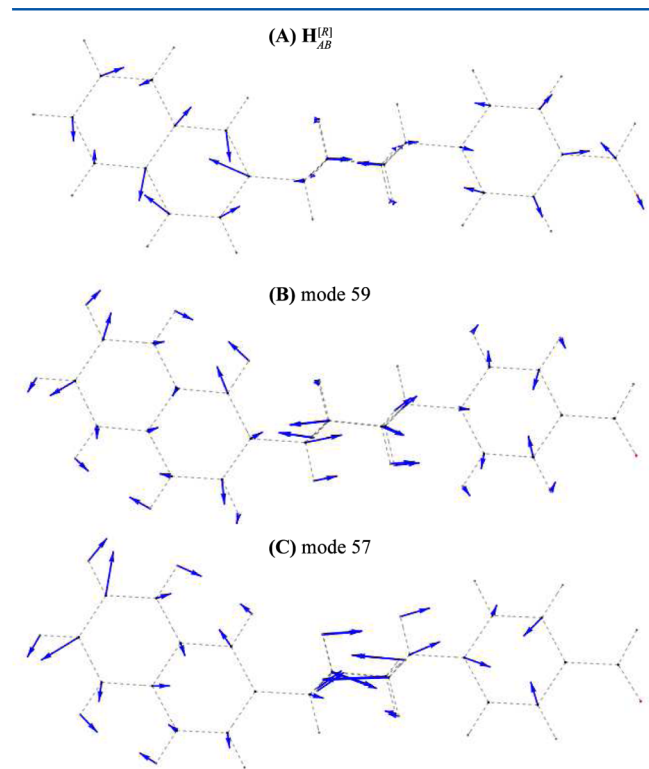


Figure 5. Quiver plot of C-1,4ee depicting the (A) diabatic coupling gradient ($H_{AB}^{[Q]}$) at $\zeta = 0$, (B) normal mode 59 from the S_0 minimum-energy configuration, and (C) normal mode 57 from the S_0 minimum-energy configuration. Those modes are each moderately rigid, with characteristic lengths of $\Delta L_{59} = 0.162 a_0$ and $\Delta L_{57} = 0.157 a_0$. At the $\zeta = 0$ geometry, the projection of the diabatic coupling gradient ($H_{AB}^{[\eta]}$) onto mode 59 is $H_{AB}^{[59]} = 45.7 \mu E_h/a_0$, and $H_{AB}^{[57]} = 34.8 \mu E_h/a_0$ for mode 57. At the $\zeta = 1$ geometry, $H_{AB}^{[59]} = 42.6 \mu E_h/a_0$, and $H_{AB}^{[57]} = 42.4 \mu E_h/a_0$. See Table 2 for a thorough description of how these quantities are determined.

Under the approximation described in this section, one can calculate the total change in diabatic coupling ($\Delta H_{AB}^{\text{total}}$) as the 2-norm of its component parts,

$$\Delta H_{AB}^{\text{total}} = \sqrt{\sum_{\eta} (\Delta H_{AB,\eta})^2} \quad (29)$$

For the $\zeta = 0$ configuration, $\Delta H_{AB}^{\text{total}} = 19 \mu E_h$, or a 87% change from the reference value. For the $\zeta = 1$ configuration, $\Delta H_{AB}^{\text{total}} = 19 \mu E_h$, a 78% change. Because of these fluctuations in the electronic coupling alone, we can expect our calculated Marcus rates to be off by up to a factor of 3 or 4 from the experimental rates. In our view, however, such small effects do not represent a significant breakdown of the Condon approximation; indeed, as a practical matter, the original calculations in ref 24 were also off by a factor of 2–3 from the experimental results. In the end,

Table 2. Analysis of the Change in Diabatic Coupling of C-1,4ee Due to Thermally Induced Conformational Fluctuations at $T = 298$ K along the Normal Modes That Contribute Most Significantly to ΔH_{AB}^a

configuration	H_{AB} (μE_h)	mode (η)	$ H_{AB}^{[\eta]} $ ($\mu E_h/a_0$)	ΔL_{η} (a_0)	$\Delta H_{AB,\eta}$ (μE_h)	$\Delta H_{AB,\eta}$ (%)
$\zeta = 0$	22.4	59	45.7	0.162	7.39	33.1
		57	34.8	0.157	5.48	24.5
		77	34.4	0.145	4.99	22.3
		106	67.8	0.072	4.91	22.0
		65	30.5	0.149	4.55	20.4
$\zeta = 1$	22.1	59	42.6	0.162	6.89	31.1
		57	42.4	0.157	6.67	30.2
		109	72.3	0.074	5.35	24.2
		73	22.1	0.177	3.91	17.7
		82	21.5	0.181	3.88	17.5

^aThe curvature around each potential energy well on the T_1 surface is taken to be the same as that of the S_0 minimum and is obtained from a ground-state Hessian calculation. Using this information, we are able to estimate how much this molecule can be expected to deviate (ΔL_{η}) from its stable configurations ($\zeta = 0$ and 1) at room temperature. Multiplying this value by the projection of the diabatic coupling gradient ($|H_{AB}^{[\eta]}|$) tells us how much we can then expect the diabatic coupling to change ($\Delta H_{AB,\eta}$) both in absolute terms and as a fraction of its value at the respective reference configuration (H_{AB}).

while there may be some fluctuations of the diabatic coupling, the molecule is rigid enough at room temperature that non-Condon effects will be relatively small.

5. DISCUSSION: THE STRICTLY DIABATIC APPROXIMATION

To test the viability of the strictly diabatic approximation described in section 3C, we have used it to calculate the Hamiltonian gradient in the BoysOV basis for C-1,4ee. To more clearly assess this approximation of a vector quantity, error analysis has been split into two components, magnitude and direction. Magnitudinal error is calculated as the conventional error for scalar quantities

$$\epsilon_{\text{mag}} = \frac{|H_{AB,\text{approx}}^{[Q]}| - |H_{AB,\text{analytic}}^{[Q]}|}{|H_{AB,\text{analytic}}^{[Q]}|} \quad (30)$$

Directional error is obtained by normalizing both the approximate and analytic vector quantities and then subtracting their inner product from unity

$$\epsilon_{\text{dir}} = 1 - \left(\frac{H_{AB,\text{approx}}^{[Q]}}{|H_{AB,\text{approx}}^{[Q]}|} \right) \cdot \left(\frac{H_{AB,\text{analytic}}^{[Q]}}{|H_{AB,\text{analytic}}^{[Q]}|} \right) \quad (31)$$

First, we discuss diabatic coupling gradients ($H_{AB}^{[Q]}$, $A \neq B$). A comparison between these results and those found for direct analytic evaluation of the diabatic coupling gradient can be found in Figure 6.

Under the strictly diabatic approximation, the diabatic coupling gradient is accurately approximated near the avoided crossing at $\zeta = 0.89$. For the region $0.8 < \zeta < 1.0$, the magnitudinal error in the diabatic coupling vector diverges linearly away from the avoided crossing, ultimately rising to 4%. In this same region, the directional error is generally much smaller; with the exception of a spike to 2% at the geometry nearest to the avoided crossing, the directional error is not greater than 0.2%. Farther away from the avoided crossing, the

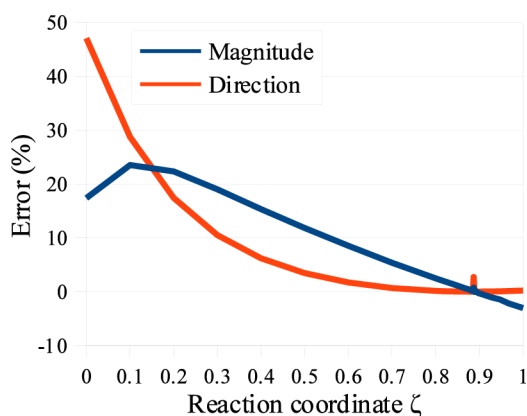


Figure 6. Error in the magnitude and direction of the diabatic coupling gradient ($H_{AB}^{[Q]}$) under the strictly diabatic approximation along the linearly interpolated reaction pathway between A^*D ($\zeta = 0$) and AD^* ($\zeta = 1$) T_1 states of the C-1,4ee molecule. Magnitudinal error is calculated as the conventional relative change for scalar quantities (eq 30). Directional error is obtained by normalizing both the approximate and analytic vector quantities and then subtracting their inner product from unity (eq 31). While both magnitudinal and directional errors are very low near the avoided crossing (at $\zeta = 0.89$), they begin to diverge significantly for $\zeta < 0.6$. While the error in the magnitude has a maximum of around 25%, the directional error is nearly 50% and rising as $\zeta \rightarrow 0$. This strongly suggests that for diabatic couplings, this approximation is only reliable where diabatization can achieve significant reductions in DC magnitudes, that is, near avoided crossings.

approximation fares much worse; for $\zeta < 0.5$, the magnitudinal error is greater than 10%, and the directional error rises to nearly 50% for $\zeta = 0$. Of course, the relatively large error at the $\zeta = 0$ configuration compared to the $\zeta = 1$ configuration reflects only the relative distance from the avoided crossing. These data strongly suggest, as one might expect, that the strictly diabatic approximation should be used only at configurations where the DC in the localized diabatic basis is significantly smaller than that in the adiabatic basis, that is, near avoided crossings (see Figure 2).

Second, we study diabatic energy gradients ($H_{AA}^{[Q]}$). In contrast to the results for the diabatic coupling gradients, the approximate diabatic state energy gradients are essentially identical to the analytic result for every point sampled. For much of configuration space, this is attributed to the fact that the dominant contribution to the diabatic energy gradient

comes from the first term on the right-hand side of eq 26, which does not depend on $U^{[Q]}$ and is therefore unchanged by the approximation. Near the avoided crossing, however, U changes rapidly, and the remaining terms in this expression can no longer be neglected. In this region, however, the DCs in the diabatic representation are smallest; therefore, the strictly diabatic approximation is the most well-founded. Thus, in two complementary limits, it seems that the strictly diabatic approximation for energy gradients can be expected to be accurate. As it turns out, the error in the approximate magnitude of the gradient is never much greater than $10^{-4}\%$, and directional error never rises above $10^{-9}\%$. For energy gradients, at least, the strictly diabatic approximation appears to be extremely robust.

6. CONCLUSIONS AND FUTURE WORK

The recent advent and implementation of analytic gradient methods for localized diabatic states has been tremendously helpful in both evaluating the reliability of these quasi-diabatic representations and increasing the functionality of these transformations. In this work, we used methods introduced in ref 30 to evaluate the properties of diabatic states of triplet–triplet energy transfer systems, finding that the DCs were negligible and that diabatic couplings were largely stable. Furthermore, we extended these methods to encompass BoysOV and GMH states. Finally, we used the knowledge that DCs in the diabatic basis are reliably small to propose an approximation that allows diabatic gradient quantities to be calculated at greatly reduced cost. We were able to show that this “strictly diabatic” approximation was successful at accurately calculating diabatic coupling gradients near avoided crossings and diabatic energy gradients everywhere. We fully expect that these results are transferable to the gradients of other observables.

Looking forward, we anticipate that the strictly diabatic approximation may make several new applications of these diabatic gradient methods more attractive. One such application is diabatic state energy minimization; because local minima on an adiabatic potential energy surface may correspond to global minima on a diabatic potential energy surface, performing a geometry optimization on diabatic surfaces may offer a more reliable way to find such configurations. We plan to implement and make available this technique in the coming months.

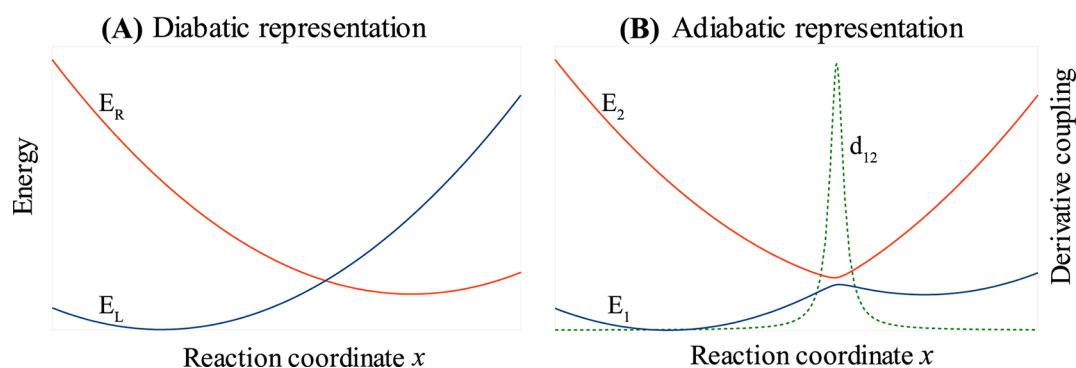


Figure 7. (A) Potential energy surfaces of a spin boson system in the diabatic representation. The DC between the two diabatic states is zero by assumption, but the diabatic coupling (not pictured) is constant with respect to the reaction coordinate x . (B) Potential energy surfaces in the adiabatic representation. The two energy surfaces no longer cross, and the diabatic coupling is now zero. The DC (d_{12}) is small except for a peak near the avoided crossing.

■ APPENDIX A. OVERVIEW OF THE SPIN BOSON MODEL

The spin boson model is a one-dimensional, two-level system that can be used to model electron and energy transfer. We will use it here as an idealized illustration of the difference between the adiabatic and strictly diabatic representations and give insight into the nature of DCs. The energy levels of the two states are given by two shifted parabolas with identical curvatures (ω), referred to here as either the left ($|\Xi_L\rangle$) or right ($|\Xi_R\rangle$) states, as depicted in Figure 7A. The diabatic coupling (V) between the states is taken to be constant as a function of the single reaction coordinate (x), so that the full Hamiltonian in atomic units is given by

$$H = T + W$$

$$= \frac{p^2}{2} \begin{pmatrix} 1 & 0 \\ 0 & 1 \end{pmatrix} + \begin{pmatrix} \frac{1}{2}\omega^2 x^2 + Mx & V \\ V & \frac{1}{2}\omega^2 x^2 - Mx + \epsilon_0 \end{pmatrix} \quad (32)$$

where p is the momentum operator, $M > 0$ defines the separation between the states in coordinate space, and $\epsilon_0 \geq 0$ is a “driving force” that defines the energy difference between the minima associated with the two states. This system is defined in the strictly diabatic basis; therefore, the DC ($d_{LR}(x) = \langle \Xi_L(x) | \partial/\partial x | \Xi_R(x) \rangle$) is zero by assumption.

One can obtain the adiabatic representation of this system, depicted in Figure 7B, by diagonalizing the potential matrix W . The resulting eigenvalue energies are given by

$$E_1(x) = \frac{1}{2}\omega^2 x^2 + \frac{\epsilon_0}{2} - \sqrt{\left(\frac{\epsilon_0}{2} - Mx\right)^2 + V^2} \quad (33)$$

and

$$E_2(x) = \frac{1}{2}\omega^2 x^2 + \frac{\epsilon_0}{2} + \sqrt{\left(\frac{\epsilon_0}{2} - Mx\right)^2 + V^2} \quad (34)$$

The corresponding adiabatic wavefunctions are given by

$$|\Phi_1(x)\rangle = \begin{pmatrix} \sqrt{\frac{1}{2} - \frac{1}{2} \frac{Mx - \epsilon_0/2}{\sqrt{(Mx - \epsilon_0/2)^2 + V^2}}} \\ -\sqrt{\frac{1}{2} + \frac{1}{2} \frac{Mx - \epsilon_0/2}{\sqrt{(Mx - \epsilon_0/2)^2 + V^2}}} \end{pmatrix} \quad (35)$$

and

$$|\Phi_2(x)\rangle = \begin{pmatrix} \sqrt{\frac{1}{2} + \frac{1}{2} \frac{Mx - \epsilon_0/2}{\sqrt{(Mx - \epsilon_0/2)^2 + V^2}}} \\ \sqrt{\frac{1}{2} - \frac{1}{2} \frac{Mx - \epsilon_0/2}{\sqrt{(Mx - \epsilon_0/2)^2 + V^2}}} \end{pmatrix} \quad (36)$$

The DC between the two adiabatic states can then be found through direct differentiation

$$d_{12}(x) = \left\langle \Phi_1(x) \left| \frac{\partial}{\partial x} \right| \Phi_2(x) \right\rangle = \frac{1}{2} \frac{MV}{(Mx - \epsilon_0/2)^2 + V^2} \quad (37)$$

Inspection of eqs 33–37 reveals a unique position— $x_{ac} = \epsilon_0/2M$ —where the energy difference between the adiabatic wavefunctions is minimized ($\Delta E(x_{ac}) = 2V$) and the derivative coupling is maximized ($d_{12}(x_{ac}) = M/2V$). This point is the avoided crossing.

■ APPENDIX B. GENERALIZATION OF BOYSOV

While the Boys representation is defined in terms of the excitation dipole matrix, X_{AB} , the BoysOV representation is defined in terms of partitions of this matrix, including the occupied component X_{AB}^{occ} and the virtual component X_{AB}^{virt} , such that their sum equals the full excitation dipole matrix, $X_{AB} = X_{AB}^{\text{occ}} + X_{AB}^{\text{virt}}$. This partitioning is trivially defined for CIS and TD-DFT/TDA because both of these methods involve only single excitations from a reference ground state (see eqs 7 and 8). For any more sophisticated wave function ansatz, however, the partitioning process is not as clear.

Although it may not always be physical, a reasonable partitioning of the dipole matrix can be defined, provided that there is a single-determinant reference ground state. For example, one can write state dipole matrix elements in the molecular orbital basis

$$X_{AB} = \sum_{r,s} X^{rs} D_{AB}^{rs} \quad (38)$$

for some excitation density matrix \mathbf{D} . The density matrix can be split into occupied and virtual components, $D_{AB}^{rs} = D_{AB}^{rs,\text{occ}} + D_{AB}^{rs,\text{virt}}$ as follows

$$D_{AB}^{rs,\text{occ}} = \begin{cases} D_{AB}^{rs} & \text{if } r, s \in \text{occ} \\ \frac{1}{2} D_{AB}^{rs} & \text{if } r \in \text{occ and } s \in \text{virt, or } s \in \text{occ and } r \in \text{virt} \\ 0 & \text{if } r, s \in \text{virt} \end{cases} \quad (39)$$

with $D_{AB}^{rs,\text{virt}}$ defined in an analogous manner. The occupied and virtual components of the dipole matrix can then be written as

$$X_{AB}^{\text{occ}} = \sum_{r,s} X^{rs} D_{AB}^{rs,\text{occ}} \quad (40)$$

and

$$X_{AB}^{\text{virt}} = \sum_{r,s} X^{rs} D_{AB}^{rs,\text{virt}} \quad (41)$$

■ AUTHOR INFORMATION

Corresponding Author

*E-mail: subotnik@sas.upenn.edu.

Notes

The authors declare no competing financial interest.

■ ACKNOWLEDGMENTS

This work was supported by NSF CAREER Grant CHE-1150851. J.E.S. acknowledges an Alfred P. Sloan Research Fellowship and a David & Lucile Packard Fellowship.

■ REFERENCES

- (1) Matsika, S.; Krause, P. Nonadiabatic Events and Conical Intersections. *Annu. Rev. Phys. Chem.* **2011**, *62*, 621–643.
- (2) Mead, C. A.; Truhlar, D. G. Conditions for the Definition of a Strictly Diabatic Electronic Basis for Molecular Systems. *J. Chem. Phys.* **1982**, *77*, 6090–6098.

- (3) Van Voorhis, T.; Kowalczyk, T.; Kaduk, B.; Wang, L.-P.; Cheng, C.-L.; Wu, Q. The Diabatic Picture of Electron Transfer, Reaction Barriers, and Molecular Dynamics. *Annu. Rev. Phys. Chem.* **2010**, *61*, 149–170.
- (4) Baer, M. Adiabatic and Diabatic Representations for Atom–Molecule Collisions: Treatment of the Collinear Arrangement. *Chem. Phys. Lett.* **1975**, *35*, 112–118.
- (5) Sadygov, R. G.; Yarkony, D. R. On the Adiabatic to Diabatic States Transformation in the Presence of a Conical Intersection: A Most Diabatic Basis from the Solution to a Poissons Equation. *J. Chem. Phys.* **1998**, *109*, 20–25.
- (6) Zhu, X.; Yarkony, D. R. Toward Eliminating the Electronic Structure Bottleneck in Nonadiabatic Dynamics on the Fly: An Algorithm to Fit Nonlocal, Quasidiabatic, Coupled Electronic State Hamiltonians Based on Ab Initio Electronic Structure Data. *J. Chem. Phys.* **2010**, *132*, 104101.
- (7) Pacher, T.; Cederbaum, L. S.; Köppel, H. In *Adiabatic and Quasidiabatic States in a Gauge Theoretical Framework*; Prigogine, I., Rice, S. A., Eds.; Advances in Chemical Physics; Wiley: New York, 1993; Vol. 84, pp 293–391.
- (8) Ruedenberg, K.; Atchity, G. J. A Quantum Chemical Determination of Diabatic States. *J. Chem. Phys.* **1993**, *99*, 3799–3803.
- (9) Atchity, G. J.; Ruedenberg, K. Determination of Diabatic States through Enforcement of Configurational Uniformity. *Theor. Chim. Acta* **1997**, *97*, 47–58.
- (10) Nakamura, H.; Truhlar, D. G. The Direct Calculation of Diabatic States Based on Configurational Uniformity. *J. Chem. Phys.* **2001**, *115*, 10353–10372.
- (11) Nakamura, H.; Truhlar, D. G. Direct Diabatization of Electronic States by the Fourfold Way. II. Dynamical Correlation and Rearrangement Processes. *J. Chem. Phys.* **2002**, *117*, 5576–5593.
- (12) Nakamura, H.; Truhlar, D. G. Extension of the Fourfold Way for Calculation of Global Diabatic Potential Energy Surfaces of Complex, Multiarrangement, Non-Born–Oppenheimer Systems: Application to HNC(S_0, S_1). *J. Chem. Phys.* **2003**, *118*, 6816–6829.
- (13) Cave, R. J.; Newton, M. D. Generalization of the Mulliken–Hush Treatment for the Calculation of Electron Transfer Matrix Elements. *Chem. Phys. Lett.* **1996**, *249*, 15–19.
- (14) Cave, R. J.; Newton, M. D. Calculation of Electronic Coupling Matrix Elements for Ground and Excited State Electron Transfer Reactions: Comparison of the Generalized Mulliken–Hush and Block Diagonalization Methods. *J. Chem. Phys.* **1997**, *106*, 9213–9226.
- (15) Yarkony, D. On the Construction of Diabatic Bases Using Molecular Properties. Rigorous Results in the Vicinity of a Conical Intersection. *J. Phys. Chem. A* **1998**, *102*, 8073–8077.
- (16) Yarkony, D. Determining the Molecular Aharonov–Bohm Phase Angle: A Rigorous Approach Employing a Molecular Properties Based Adiabatic to Diabatic States Transformation. *J. Chem. Phys.* **1999**, *110*, 701–705.
- (17) Kryachko, E. S.; Yarkony, D. R. Diabatic Bases and Molecular Properties. *Int. J. Quantum Chem.* **2000**, *76*, 235–243.
- (18) Voityuk, A. A.; Rösch, N. Fragment Charge Difference Method for Estimating Donor–Acceptor Electronic Coupling: Application to DNA π -Stacks. *J. Chem. Phys.* **2002**, *117*, 5607–5616.
- (19) Hsu, C.-P.; You, Z.-Q.; Chen, H.-C. Characterization of the Short-Range Couplings in Excitation Energy Transfer. *J. Phys. Chem. C* **2008**, *112*, 1204–1212.
- (20) Chen, H.-C.; You, Z.-Q.; Hsu, C.-P. The Mediated Excitation Energy Transfer: Effects of Bridge Polarizability. *J. Chem. Phys.* **2008**, *129*, 084708.
- (21) Hsu, C.-P. The Electronic Couplings in Electron Transfer and Excitation Energy Transfer. *Acc. Chem. Res.* **2009**, *42*, 509–518.
- (22) Subotnik, J. E.; Yeganeh, S.; Cave, R. J.; Ratner, M. A. Constructing Diabatic States from Adiabatic States: Extending Generalized Mulliken–Hush to Multiple Charge Centers with Boys Localization. *J. Chem. Phys.* **2008**, *129*, 244101.
- (23) Subotnik, J. E.; Cave, R. J.; Steele, R. P.; Shenvi, N. The Initial and Final States of Electron and Energy Transfer Processes: Diabatization As Motivated by System–Solvent Interactions. *J. Chem. Phys.* **2009**, *130*, 234102.
- (24) Subotnik, J. E.; Vura-Weis, J.; Sodt, A. J.; Ratner, M. A. Predicting Accurate Electronic Excitation Transfer Rates via Marcus Theory with Boys or Edmiston–Ruedenberg Localized Diabatization. *J. Phys. Chem. A* **2010**, *114*, 8665–8675.
- (25) Wu, Q.; Van Voorhis, T. Direct Calculation of Electron Transfer Parameters through Constrained Density Functional Theory. *J. Phys. Chem. A* **2006**, *110*, 9212–9218.
- (26) Wu, Q.; Voorhis, T. V. Extracting Electron Transfer Coupling Elements from Constrained Density Functional Theory. *J. Chem. Phys.* **2006**, *125*, 164105.
- (27) Wu, Q.; Van Voorhis, T. Constrained Density Functional Theory and Its Application in Long-Range Electron Transfer. *J. Chem. Theory Comput.* **2006**, *2*, 765–774.
- (28) Newton, M. D. Quantum Chemical Probes of Electron-Transfer Kinetics: The Nature of Donor–Acceptor Interactions. *Chem. Rev.* **1991**, *91*, 767–792.
- (29) Alguire, E.; Subotnik, J. E. Optimal Diabatic States Based on Solvation Parameters. *J. Chem. Phys.* **2012**, *137*, 194108.
- (30) Fatehi, S.; Alguire, E.; Subotnik, J. E. Derivative Couplings and Analytic Gradients for Diabatic States, With an Implementation for Boys-Localized Configuration-Interaction Singles. *J. Chem. Phys.* **2013**, *139*, 124112.
- (31) Granucci, G.; Persico, M.; Toniolo, A. Direct Semiclassical Simulation of Photochemical Processes with Semiempirical Wave Functions. *J. Chem. Phys.* **2001**, *114*, 10608–10615.
- (32) Plasser, F.; Granucci, G.; Pittner, J.; Barbatti, M.; Persico, M.; Lischka, H. Surface Hopping Dynamics Using a Locally Diabatic Formalism: Charge Transfer in the Ethylene Dimer Cation and Excited State Dynamics in the 2-Pyridone Dimer. *J. Chem. Phys.* **2012**, *137*, 22A514.
- (33) Tully, J. C. Molecular Dynamics with Electronic Transitions. *J. Chem. Phys.* **1990**, *93*, 1061–1071.
- (34) Kapral, R.; Ciccotti, G. Mixed Quantum–Classical Dynamics. *J. Chem. Phys.* **1999**, *110*, 8919–8929.
- (35) Ben-Nun, M.; Martinez, T. J. A Multiple Spawning Approach to Tunneling Dynamics. *J. Chem. Phys.* **2000**, *112*, 6113–6121.
- (36) Ananth, N.; Venkataraman, C.; Miller, W. H. Semiclassical Description of Electronically Nonadiabatic Dynamics via the Initial Value Representation. *J. Chem. Phys.* **2007**, *127*, 084114.
- (37) Closs, G. L.; Piotrowiak, P.; MacInnis, J. M.; Fleming, G. R. Determination of Long-Distance Intramolecular Triplet Energy-Transfer Rates. Quantitative Comparison with Electron Transfer. *J. Am. Chem. Soc.* **1988**, *110*, 2652–2653.
- (38) Closs, G. L.; Johnson, M. D.; Miller, J. R.; Piotrowiak, P. A Connection between Intramolecular Long-Range Electron, Hole, and Triplet Energy Transfers. *J. Am. Chem. Soc.* **1989**, *111*, 3751–3753.
- (39) Fatehi, S.; Alguire, E.; Shao, Y.; Subotnik, J. E. Analytic Derivative Couplings between Configuration-Interaction-Singles States with Built-in Electron-Translation Factors for Translational Invariance. *J. Chem. Phys.* **2011**, *135*, 234105.
- (40) Lengsfeld, B. H.; Yarkony, D. R. On the Evaluation of Nonadiabatic Coupling Matrix Elements for MCSCF/CI Wave Functions Using Analytic Derivative Methods. III. Second Derivative Terms. *J. Chem. Phys.* **1986**, *84*, 348.
- (41) Saxe, P.; Yarkony, D. R. On the Evaluation of Nonadiabatic Coupling Matrix Elements for MCSCF/CI Wave Functions. IV. Second Derivative Terms Using Analytic Gradient Methods. *J. Chem. Phys.* **1987**, *86*, 321.
- (42) Lengsfeld, B. H.; Yarkony, D. R. Nonadiabatic Interactions between Potential Energy Surfaces — Theory and Applications. *Adv. Chem. Phys.* **1992**, *82*, 1–71.
- (43) Yarkony, D. R. *Conical Intersections in Electron Photodetachment Spectroscopy: Theory and Applications*; Advanced Series in Physical Chemistry; World Scientific: River Edge, NJ; 2004; Vol. 15, pp 129–174.
- (44) Lengsfeld, B. H.; Saxe, P.; Yarkony, D. R. On the Evaluation of Nonadiabatic Coupling Matrix Elements Using SA-MCSCF/CI Wave

Functions and Analytic Gradient Methods. I. *J. Chem. Phys.* **1984**, *81*, 4549–4553.

(45) Saxe, P.; Lengsfeld, B. H., III; Yarkony, D. R. On the Evaluation of Non-Adiabatic Coupling Matrix Elements for Large Scale {CI} Wavefunctions. *Chem. Phys. Lett.* **1985**, *113*, 159–164.

(46) Lischka, H.; Dallos, M.; Shepard, R. Analytic MRCI Gradient for Excited States: Formalism and Application to the n-Valence- and n-(3s,3p) Rydberg States of Formaldehyde. *Mol. Phys.* **2002**, *100*, 1647–1658.

(47) Lischka, H.; Dallos, M.; Szalay, P. G.; Yarkony, D. R.; Shepard, R. Analytic Evaluation of Nonadiabatic Coupling Terms at the MR-CI Level. I. Formalism. *J. Chem. Phys.* **2004**, *120*, 7322–7329.

(48) Dallos, M.; Lischka, H.; Shepard, R.; Yarkony, D. R.; Szalay, P. G. Analytic Evaluation of Nonadiabatic Coupling Terms at the MR-CI level. II. Minima on the Crossing Seam: Formaldehyde and the Photodimerization of Ethylene. *J. Chem. Phys.* **2004**, *120*, 7330–7339.

(49) Jorgensen, P.; Simons, J. Ab Initio Analytical Molecular Gradients and Hessians. *J. Chem. Phys.* **1983**, *79*, 334–357.

(50) Helgaker, T. U.; Almlöf, J. A Second-Quantization Approach to the Analytical Evaluation of Response Properties for Perturbation-Dependent Basis Sets. *Int. J. Quantum Chem.* **1984**, *26*, 275–291.

(51) Page, M.; Saxe, P.; Adams, G. F.; Lengsfeld, B. H. Multireference CI Gradients and MCSCF Second Derivatives. *J. Chem. Phys.* **1984**, *81*, 434–439.

(52) Shepard, R. Geometrical Energy Derivative Evaluation with MRCI Wave Functions. *Int. J. Quantum Chem.* **1987**, *31*, 33–44.

(53) Shepard, R.; Lischka, H.; Szalay, P. G.; Kovar, T.; Ernzerhof, M. A General Multireference Configuration Interaction Gradient Program. *J. Chem. Phys.* **1992**, *96*, 2085–2098.

(54) Shao, Y.; Molnar, L. F.; Jung, Y.; Kussmann, J.; Ochsenfeld, C.; Brown, S. T.; Gilbert, A. T.; Slipchenko, L. V.; Levchenko, S. V.; O'Neill, D. P.; et al. Advances in Methods and Algorithms in a Modern Quantum Chemistry Program Package. *Phys. Chem. Chem. Phys.* **2006**, *8*, 3172–3191.

(55) Krylov, A. I.; Gill, P. M. W. Q-Chem: An Engine for Innovation. *WIREs Comput. Mol. Sci.* **2013**, *3*, 317–326.

(56) Nitzan, A. *Chemical Dynamics in Condensed Phases*; Oxford University Press: New York, 2006.

(57) Ratner, M.; Schatz, G. *Quantum Mechanics in Chemistry*; Dover Publications: Mineola, NY, 2002.